

# Generic Contrast Agents

Our portfolio is growing to serve you better. Now you have a *choice*.



[VIEW CATALOG](#)

# AJNR

This information is current as of May 6, 2025.

## **Arterial Spin-Labeling and DSC Perfusion Metrics Improve Agreement in Neuroradiologists' Clinical Interpretations of Posttreatment High-Grade Glioma Surveillance MR Imaging—An Institutional Experience**

Ghiam Yamin, Eric Tranvinh, Bryan A. Lanzman, Elizabeth Tong, Syed S. Hashmi, Chirag B. Patel and Michael Iv

*AJNR Am J Neuroradiol* 2024, 45 (4) 453-460

doi: <https://doi.org/10.3174/ajnr.A8190>

<http://www.ajnr.org/content/45/4/453>

# Arterial Spin-Labeling and DSC Perfusion Metrics Improve Agreement in Neuroradiologists' Clinical Interpretations of Posttreatment High-Grade Glioma Surveillance MR Imaging—An Institutional Experience

 Ghiam Yamin,  Eric Tranvinh,  Bryan A. Lanzman,  Elizabeth Tong,  Syed S. Hashmi,  Chirag B. Patel, and  Michael Iv



## ABSTRACT

**BACKGROUND AND PURPOSE:** MR perfusion has shown value in the evaluation of posttreatment high-grade gliomas, but few studies have shown its impact on the consistency and confidence of neuroradiologists' interpretation in routine clinical practice. We evaluated the impact of adding MR perfusion metrics to conventional contrast-enhanced MR imaging in posttreatment high-grade glioma surveillance imaging.

**MATERIALS AND METHODS:** This retrospective study included 45 adults with high-grade gliomas who had posttreatment perfusion MR imaging. Four neuroradiologists assigned Brain Tumor Reporting and Data System scores for each examination on the basis of the interpretation of contrast-enhanced MR imaging and then after the addition of arterial spin-labeling-CBF, DSC-relative CBV, and DSC-fractional tumor burden. Interrater agreement and rater agreement with a multidisciplinary consensus group were assessed with  $\kappa$  statistics. Raters used a 5-point Likert scale to report confidence scores. The frequency of clinically meaningful score changes resulting from the addition of each perfusion metric was determined.

**RESULTS:** Interrater agreement was moderate for contrast-enhanced MR imaging alone ( $\kappa = 0.63$ ) and higher with perfusion metrics (arterial spin-labeling-CBF,  $\kappa = 0.67$ ; DSC-relative CBV,  $\kappa = 0.66$ ; DSC-fractional tumor burden,  $\kappa = 0.70$ ). Agreement between raters and consensus was highest with DSC-fractional tumor burden ( $\kappa = 0.66$ – $0.80$ ). Confidence scores were highest with DSC-fractional tumor burden. Across all raters, the addition of perfusion resulted in clinically meaningful interpretation changes in 2%–20% of patients compared with contrast-enhanced MR imaging alone.

**CONCLUSIONS:** Adding perfusion to contrast-enhanced MR imaging improved interrater agreement, rater agreement with consensus, and rater confidence in the interpretation of posttreatment high-grade glioma MR imaging, with the highest agreement and confidence scores seen with DSC-fractional tumor burden. Perfusion MR imaging also resulted in interpretation changes that could change therapeutic management in up to 20% of patients.

**ABBREVIATIONS:** ASL = arterial spin-labeling; BT-RADS = Brain Tumor Reporting and Data System; CE = contrast-enhanced; CRT = chemoradiotherapy; FTB = fractional tumor burden; GBM = glioblastoma; HGG = high-grade glioma; IRA = interrater agreement; rCBV = relative CBV

Surveillance MR imaging following surgery and chemoradiotherapy (CRT) is integral to the care of patients with high-grade gliomas (HGGs). In the Response Assessment in Neuro-Oncology criteria, the assessment of tumor status is based on

changes in contrast-enhanced (CE) T1-weighted images and T2 FLAIR signal across time, taking into consideration clinical factors such as functional status, interscan therapy, and time since completion of CRT.<sup>1,2</sup> However, interpretation of posttreatment HGG MR imaging is often challenging because of the overlapping imaging findings between tumor progression and CRT effects.


Perfusion metrics are not yet universally included in the assessment, in part due to a perceived lack of standardization and validation, but studies have shown them to be valuable in the evaluation of posttreatment HGGs. DSC perfusion-derived relative CBV (rCBV), which is the most widely used perfusion metric in brain tumor imaging, is a biomarker for tumor angiogenesis and can distinguish HGG recurrence from radiation effects.<sup>3–5</sup> Arterial spin-labeling (ASL) perfusion-derived CBF has also been shown to be higher in recurrent HGGs than in treatment-related

Received July 6, 2023; accepted after revision November 16.

From the Department of Radiology (G.Y., E. Tranvinh, B.A.L., E. Tong, S.S.H., M.I.), Division of Neuroimaging and Neurointervention, Stanford University Medical Center, Stanford, California; and Department of Neuro-Oncology (C.B.P.), The University of Texas MD Anderson Cancer Center, Houston, Texas.

Ghiam Yamin and Eric Tranvinh are co-first authors and contributed equally to this work.

Please address correspondence to Michael Iv, MD, Stanford University Medical Center, Center for Academic Medicine, Radiology +; MC: 5659, Room 323A, 453 Quarry Rd, Palo Alto, CA 94304; e-mail: miv@stanford.edu; @Michael\_Iv\_MD

 Indicates open access to non-subscribers at [www.ajnr.org](http://www.ajnr.org)

<http://dx.doi.org/10.3174/ajnr.A8190>

effects and correlates well with DSC-derived rCBV.<sup>6-8</sup> DSC perfusion-derived fractional tumor burden (FTB) can delineate areas of low, intermediate, and high likelihood of tumor burden within a contrast-enhancing volume on the basis of predefined rCBV thresholds.<sup>9</sup> Fewer studies, however, have shown the positive clinical impact of adding MR perfusion to conventional CE-MR imaging in the assessment of posttreatment HGG surveillance imaging in real-time practice. Geer et al<sup>10</sup> showed that the addition of perfusion metrics to CE-MR imaging changed the management plan in 8.5% of patients and increased confidence in the management plan by 57.6%. Iv et al<sup>9</sup> showed that the addition of FTB can influence clinical decision-making among a panel of physicians involved in the care of patients with gliomas.

In this study, we investigated the impact of adding ASL-derived CBF, DSC-derived rCBV, and DSC-derived FTB to conventional CE-MR imaging on neuroradiologists' clinical interpretations of posttreatment MR imaging of HGGs. We hypothesized that the addition of perfusion metrics would improve interrater agreement (IRA) among neuroradiologists and between neuroradiologists and an experienced multidisciplinary group, improve confidence in interpretation, and yield clinically meaningful changes in interpretation.

## MATERIALS AND METHODS

### Patients

This retrospective study was approved by the Stanford University institutional review board. The records of patients with treated HGGs who had MR imaging performed between May 2019 and December 2019 were reviewed. Inclusion criteria were as follows: 1) 18 years of age or older; 2) pathologically proved *IDH* wild-type HGG (we used the integrated tumor diagnosis from the time of the original histopathologic evaluation); 3) prior treatment with surgical resection followed by CRT; and 4) posttreatment MR imaging with ASL and DSC. For each patient, the first MR images with complete ASL and DSC acquisitions and postprocessed imaging data were selected. Patients were excluded if either the perfusion imaging set was incomplete or the contrast-enhancing lesion was not located within the brain parenchyma. *IDH*-mutant gliomas were also excluded because their biology is different from that of *IDH* wild-type glioblastomas (GBM). Clinical and histopathologic information was obtained through the electronic medical records.

### MR Imaging Acquisition

MR imaging was performed on 1.5T (Signa Explorer; GE Healthcare) and 3T (Discovery MR750; GE Healthcare) scanners using our institutional glioma-specific MR imaging protocol. While this protocol has undergone slight changes with time, the sequences relevant to this study have remained constant: 3D T1 fast-spoiled gradient recalled-echo brain volume (BRAVO), 3D T2 FLAIR, ASL, DSC, axial T2, and 3D T1 BRAVO postcontrast images.

ASL was performed using pseudocontinuous labeling with the following parameters: TR/TE/label time/postlabel delay = 5500/2.5/1500/2000 ms, 3D background-suppressed fast-spin-echo stack-of-spirals readout, and 4-mm in-plane and 6-mm through-plane

resolution. ASL postprocessing was performed by an automated reconstruction script that sent CBF images to PACS.

Before acquisition of DSC perfusion images, a 0.05-mmol/kg dose of gadobenate dimeglumine was administered as a preload to help correct for leakage effects.<sup>11</sup> DSC perfusion was performed with a 4-mL/s bolus of 0.05-mmol/kg gadobenate dimeglumine and single-echo gradient-echo-planar imaging using the following parameters: TR/TE = 1800/35–40 ms, section thickness = 5 mm, no interslice gaps with 20 slices covering the brain, flip angle = 30°, matrix = 128 × 128 mm, FOV = 240 mm.

### DSC Image Processing

DSC perfusion images were postprocessed by our 3D and Quantitative Imaging Laboratory at a workstation equipped with Aycan (Version 3.16.002) and IB Neuro (Version 2.0; Imaging Biometrics), a commercially available image-processing plug-in that implements a leakage-correction algorithm and generates standardized rCBV and FTB maps.<sup>12-16</sup> Semiautomated image segmentation and processing were performed with IB Rad Tech (Version 2.0; Imaging Biometrics), a workflow engine that generates quantitative  $\Delta$  T1 and FTB maps from the IB Delta Suite (Version 2.0; Imaging Biometrics) and IB Neuro plug-in. This workflow has been described in detail previously.<sup>9,16</sup> Two standardized rCBV thresholds (1 and 1.56) were used to define 3 FTB classes: FTB<sub>low</sub>, percentage of contrast-enhancing voxels with rCBV  $\leq 1.0$ ; FTB<sub>mid</sub>, percentage of voxels with rCBV between 1.0 and 1.56; and FTB<sub>high</sub>, percentage of voxels with rCBV of  $\geq 1.56$ . A standardized rCBV value of 1.56 was used as the higher threshold for tumor prediction considering our own clinical experience and a prior report of this value indicating >88% probability of tumor.<sup>17</sup> Mean and median rCBV values of the contrast-enhancing volumes were generated for each patient. Volumetric images of the contrast-enhancing lesion superimposed on the FTB map containing colored voxels of each class (FTB<sub>low</sub> = blue; FTB<sub>mid</sub> = yellow; FTB<sub>high</sub> = red) and a histogram displaying voxels for the entire contrast-enhancing volume were also produced.

### MR Imaging Interpretation and Brain Tumor Reporting and Data System Scoring

Studies were interpreted by 4 neuroradiology faculty with 1 (E. Tong), 3 (S.S.H.), 4 (B.A.L.) and 6 (E. Tranvinh) years of practice experience following 1 year of a dedicated neuroradiology fellowship at the time of the study. The 2 raters with fewer experience years also had less experience with perfusion imaging than the other 2 raters. Each rater was provided a worklist of 45 de-identified patients in PACS, including the MR imaging of interest and 2 of the most recent prior MR images for comparison, during 1 session. Clinical information such as tumor histology and molecular status and a brief treatment course was also provided. For each patient, raters provided scores using the Brain Tumor Reporting and Data System (BT-RADS).<sup>2</sup> In BT-RADS, MR imaging is assigned a score from 0 to 4 based on changes in the contrast-enhancing lesion and T2 FLAIR signal compared with the most recent prior MR imaging, taking into consideration the time since completion of CRT and treatment with adjuvant medications such as bevacizumab and steroids: 0, baseline; 1a, improving imaging findings due to decreased tumor burden and/or treatment

effect; 1b, improving imaging findings due to bevacizumab or steroids; 2, no change; 3a, worsening imaging findings thought to represent treatment effects; 3b, worsening imaging findings representing an indeterminate mix of tumor and treatment effects; 3c, worsening imaging findings thought to represent increasing tumor burden; and 4, worsening imaging findings highly suspicious for tumor progression.

Considering minor differences between the following pairs of scores in their influence on patient management, BT-RADS scores 1a and 1b were combined into a single 1a/b category and scores 3c and 4 were combined into a single 3c/4 category to facilitate the determination of whether the addition of perfusion imaging resulted in clinically meaningful changes in interpretation. A clinically meaningful change in interpretation was defined as a change in score from  $\leq 3a$  to  $\geq 3b$  (and vice versa) and from  $\leq 3b$  to 3c/4 (and vice versa), because these changes reflected a change in the proportion and confidence of predicted tumor burden. BT-RADS scores are associated with management recommendations, and the higher the predicted tumor burden, the more likely it is that there will be a recommended change in management.<sup>2</sup> In practice, the stability or worsening of clinical symptoms may also help to guide the management. Often, worsening clinical symptoms coupled with worsening imaging findings, particularly if there is any tumor concern (eg, score of  $\geq 3b$ ), may favor an earlier change in management (eg, administration of steroids or bevacizumab or surgical resection) over just shortening the surveillance imaging time.

Each rater provided an initial BT-RADS score based only on conventional CE-MR imaging before any perfusion maps were evaluated. In the same session, each rater then provided additional scores after reviewing each of the ASL-CBF, DSC-rCBV, and DSC-FTB maps. The order in which the perfusion maps were reviewed was randomized from patient to patient by a study member not involved in image interpretation and scoring (G.Y.). This process resulted in a total of 4 scores per patient. Quantitative and qualitative imaging data were provided for DSC-rCBV and DSC-FTB as previously mentioned. Quantitative values were not available for ASL-CBF, reflecting the lack of a clinically validated threshold for differentiating tumor and treatment effect. Raters then provided a confidence score for each BT-RADS assessment. Confidence scores were based on a 5-point Likert scale (1, not confident; 2, less confident; 3, average confidence; 4, more confident; and 5, very confident).

### Reference Standard

Because histopathology was not available at each MR imaging timepoint, a reference standard BT-RADS score was determined for each patient by an experienced multidisciplinary consensus group comprising a board-certified neuroradiologist with 8 years of postfellowship experience (M.I.) and a board-eligible neuro-oncologist (C.B.P.), both of whom attend our institution's weekly neuro-oncology tumor board and are regularly involved in patient care-related decision-making. They each assessed the MR imaging, including perfusion data, relevant priors, and clinical information. If there was disagreement, follow-up MR imaging and any available pathology results during the

**Table 1: Patient demographics**

Demographics	
Age (yr)	
Mean (SD)	61 (13)
Range	31–88
Sex	
Male	25 (56%)
Female	20 (44%)
Integrated diagnosis	
GBM, <i>IDH</i> wild-type, WHO 4	44 (98%)
Astrocytoma, <i>IDH</i> wild-type, WHO 3	1 (2%)
HGG molecular features	
<i>IDH</i> wild-type	45 (100%)
<i>MGMT</i> promoter-unmethylated	24 (53%)
<i>MGMT</i> promoter-methylated	19 (42%)
Unknown <i>MGMT</i> promoter methylation status	2 (4%)

**Note:**—WHO indicates World Health Organization.

follow-up period were reviewed to determine a single consensus score.

### Statistical Analysis

The IRA among the 4 raters was determined using the Fleiss  $\kappa$ . Agreement between the consensus and each rater's scores was assessed using the Cohen  $\kappa$ . The strength of agreement was interpreted using the following scale:  $<0.2$ , poor; 0.2–0.39, slight; 0.4–0.59, fair; 0.6–0.79, moderate; 0.8–0.99, substantial; 1, perfect. The Kruskal-Wallis test was used to evaluate whether ASL-CBF, DSC-rCBV, and DSC-FTB when added to CE-MR imaging had an effect on the number of clinically meaningful score changes. Randomizing the order of perfusion map interpretations made observations in each group and between groups independent. Descriptive statistics were used to evaluate raters' confidence in the BT-RADS scoring. While confidence scores were assessed with an ordinal scale (Likert scale), the mean of scores was calculated to interpret trends; in other words, for clarity of interpretation, we treated the scale as an approximation to an interval scale. In addition, for each rater, the Friedman test was used to determine whether there was a difference in confidence scores among the dependent variables of CE-MR imaging, CE-MR imaging+ASL-CBF, CE-MR imaging+DSC-rCBV, and CE-MR imaging+DSC-FTB. The post hoc Dunn-Bonferroni test was performed to detect pair-wise differences among groups. For all analyses,  $P < .05$  was considered significant. Statistical analyses were performed with the DATAtab online Statistics Calculator (<http://www.datatab.net>).

## RESULTS

### Patients

Ninety-three MR imaging examinations were eligible for the study. Thirty-one MR imaging examinations were excluded because they were follow-up examinations of patients already included in the study, leaving 62 unique patient examinations. Ten examinations were excluded for lack of postprocessed DSC data, and 1 was excluded for lack of ASL. One patient was excluded because the enhancing lesion was outside the brain parenchyma. Five *IDH*-mutant tumors were excluded from the analysis. The final cohort consisted of 45 patients (25 men, 20 women; mean age, 61 [SD, 13] years; range, 31–88 years) (Table 1). Of 45 HGGs, 44 were *IDH* wild-type grade 4 GBMs, and 1



was an *IDH* wild-type grade 3 astrocytoma. The median number of days between the first histologic diagnosis and the perfusion MR imaging assessed was 296 days (range, 70–2777 days).

#### Agreement in MR Imaging Interpretation among Raters

The IRA was 0.63 (95% CI, 0.56–0.69;  $P < .001$ ) for CE-MR imaging alone; 0.67 (95% CI, 0.60–0.74;  $P < .001$ ) for CE-MR imaging+ASL-CBF; 0.66 (95% CI, 0.60–0.73;  $P < .001$ ) for CE-MR imaging+DSC-rCBV; and 0.70 (95% CI, 0.63–0.77;  $P < .001$ ) for CE-MR imaging+DSC-FTB (Table 2). Figures 1 and 2 show BT-RADS scores by raters and consensus in representative patients with posttreatment GBMs on surveillance MR imaging.

#### Agreement in MR Imaging Interpretation between the Multidisciplinary Consensus Group and Raters

Scores from the consensus group yielded 10 patients with a BT-RADS score of 1a/1b, 9 with a score of 2, one with a score of 3a,

four with a score of 3b, and 21 with a score of 3c/4. None were assigned a score of 0.

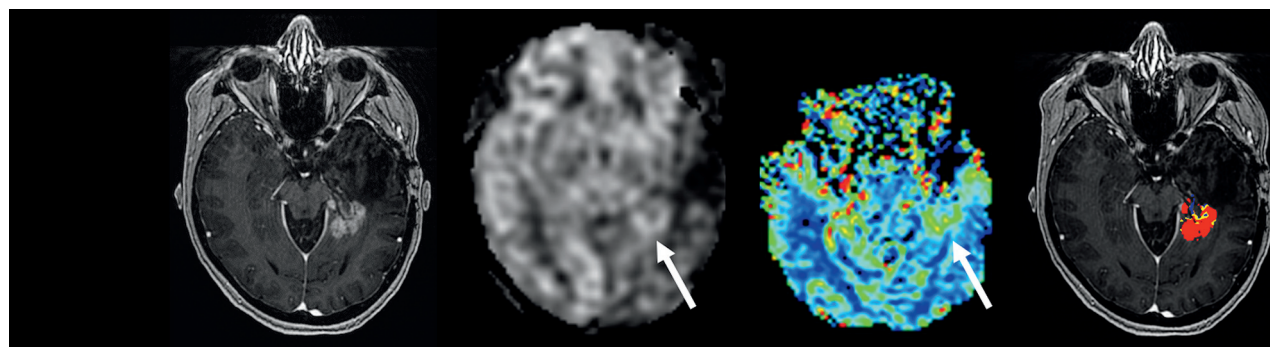
The Cohen  $\kappa$  was used to determine agreement between consensus and individual raters' scores (Table 3). For rater 1,  $\kappa$  scores for CE-MR imaging alone, CE-MR imaging+ASL-CBF, CE-MR imaging+DSC-rCBV, and CE-MR imaging+DSC-FTB were 0.53 (95% CI, 0.31–0.75), 0.58 (95% CI, 0.36–0.80), 0.58 (95% CI, 0.36–0.80), and 0.66 (95% CI, 0.46–0.87), respectively. For rater 2,  $\kappa$  scores were 0.70 (95% CI, 0.50–0.91), 0.69 (95% CI, 0.48–0.89), 0.71 (95% CI, 0.51–0.90), and 0.80 (95% CI, 0.63–0.97), respectively. For rater 3,  $\kappa$  scores were 0.63 (95% CI, 0.43–0.84), 0.61 (95% CI, 0.39–0.82), 0.63 (95% CI, 0.42–0.84), and 0.66 (95% CI, 0.46–0.86), respectively. For rater 4,  $\kappa$  scores were 0.58 (95% CI, 0.36–0.80), 0.65 (95% CI, 0.44–0.86), 0.68 (95% CI, 0.47–0.88), and 0.73 (95% CI, 0.55–0.92), respectively. All analyses showed  $P < .001$ .

#### Clinically Meaningful Changes in BT-RADS Scores with Perfusion Imaging

The number of clinically meaningful score changes following the addition of perfusion metrics relative to conventional CE-MR imaging alone is shown in Table 4 and illustrated in Fig 3. For rater 1, the number of score changes occurred in 11% (5/45) of patients with CE-MR imaging+ASL-CBF, 11% (5/45) with CE-MR imaging+DSC-rCBV, and 18% (8/45) with CE-MR imaging+DSC-FTB. For rater 2, the number of score changes

**Table 2: Agreement in MR imaging interpretation among 4 neuroradiologists**

	Fleiss $\kappa$	95% CI	P Value
Conventional CE-MR imaging	0.63	0.56–0.69	<.001
CE-MR imaging + ASL-CBF	0.67	0.60–0.74	<.001
CE-MR imaging + DSC-rCBV	0.66	0.60–0.73	<.001
CE-MR imaging + DSC-FTB	0.70	0.63–0.77	<.001



Rater	CE-MRI	CE-MRI + ASL-CBF	CE-MRI + DSC-rCBV	CE-MRI + DSC-FTB
1	3b	3c/4	3c/4	3c/4
2	3b	3b	3b	3c/4
3	3b	3c/4	3c/4	3c/4
4	3b	3c/4	3c/4	3c/4
Consensus	3c/4			

**FIG 1.** Example of rater BT-RADS scores in a 57-year-old woman with previously treated GBM and worsening findings on surveillance MR imaging. The T1 postgadolinium image demonstrates an enhancing lesion in the left mesial temporal lobe. The lesion has elevated ASL-CBF and DSC-rCBV (white arrows). The DSC-FTB image shows that the enhancing voxels are in the “high” fractional tumor burden (red voxels) category. The addition of perfusion metrics to CE-MR imaging resulted in a scoring upgrade from 3b (worsening imaging findings, indeterminate mix of treatment effects and tumor) to 3c/4 (likely tumor progression) across all raters and agreed with the consensus score of 3c/4. For 3 of 4 raters, the upgrade occurred with all perfusion metrics, and for rater 2, it occurred only with DSC-FTB.

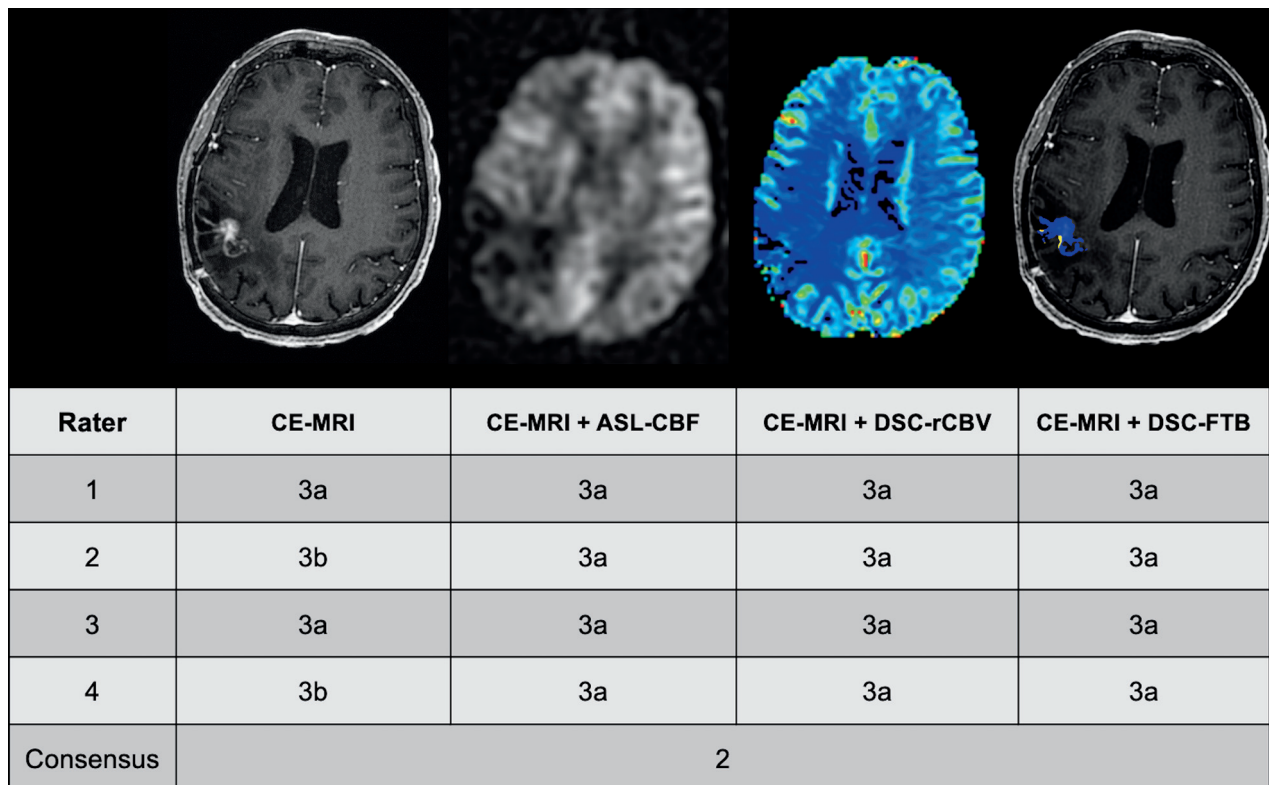


**FIG 2.** Example of rater BT-RADS scores in a 61-year-old woman with previously treated GBM and equivocally worsening findings on surveillance MR imaging. The T1 postgadolinium image demonstrates an enhancing lesion in the right temporal lobe. The lesion shows no elevated ASL-CBF or DSC-rCBV, and DSC-FTB shows that the enhancing voxels are in the “low” FTB (blue voxels) category. For two raters, the addition of perfusion metrics to CE-MR imaging resulted in a scoring downgrade from 3b (worsening imaging findings, indeterminate mix of treatment effects and tumor) to 3a (worsening imaging findings, likely treatment effects). For the other raters, perfusion metrics did not influence their assessment. The consensus score in this case was 2 (no change). The discrepancy between the consensus group and the raters was due to differences in opinion as to whether the enhancing lesion had subtly increased in size from the prior MR imaging (not shown).

**Table 3: Agreement in MR imaging interpretation between an experienced multidisciplinary consensus group and each of 4 neuroradiologists<sup>a</sup>**

	More Experienced		Less Experienced	
	Rater 1	Rater 2	Rater 3	Rater 4
Conventional CE-MR imaging	0.53 (0.31–0.75)	0.70 (0.50–0.91)	0.63 (0.43–0.84)	0.58 (0.36–0.80)
CE-MR imaging + ASL-CBF	0.58 (0.36–0.80)	0.69 (0.48–0.89)	0.61 (0.39–0.82)	0.65 (0.44–0.86)
CE-MR imaging + DSC-rCBV	0.58 (0.36–0.80)	0.71 (0.51–0.90)	0.63 (0.42–0.84)	0.68 (0.47–0.88)
CE-MR imaging + DSC-FTB	0.66 (0.46–0.87)	0.80 (0.63–0.97)	0.66 (0.46–0.86)	0.73 (0.55–0.92)

<sup>a</sup> All analyses showed  $P < .001$ . Values are Cohen  $\kappa$  with 95% confidence intervals in the parentheses.

**Table 4: Frequency of clinically meaningful changes in BT-RADS scores in 45 patients following the inclusion of perfusion metrics compared with conventional CE-MR imaging alone<sup>a</sup>**

	More Experienced		Less Experienced	
	Rater 1	Rater 2	Rater 3	Rater 4
CE-MR imaging + ASL-CBF	5 (11%)	7 (16%)	1 (2%)	7 (16%)
CE-MR imaging + DSC-rCBV	5 (11%)	4 (9%)	2 (4%)	8 (18%)
CE-MR imaging + DSC-FTB	8 (18%)	6 (13%)	3 (7%)	9 (20%)

<sup>a</sup> No significance was found among ASL-CBF, DSC-rCBV, and DSC-FTB when added to CE-MR imaging with respect to the number of clinically meaningful score changes ( $P = .53$ ). Percentages are in parentheses.

occurred in 16% (7/45), 9% (4/45), and 13% (6/45) of patients, respectively. For rater 3, the number of score changes occurred in 2% (1/45), 4% (2/45), and 7% (3/45) of patients, respectively. For rater 4, the number of score changes occurred in 16% (7/45), 18% (8/45), and 20% (9/45) of patients, respectively.

The range of clinically meaningful changes across all 4 raters was 2%–20%. No significance was found among ASL-CBF, DSC-rCBV, and DSC-FTB when added to CE-MR imaging with respect to the number of clinically meaningful changes ( $P = .53$ ).

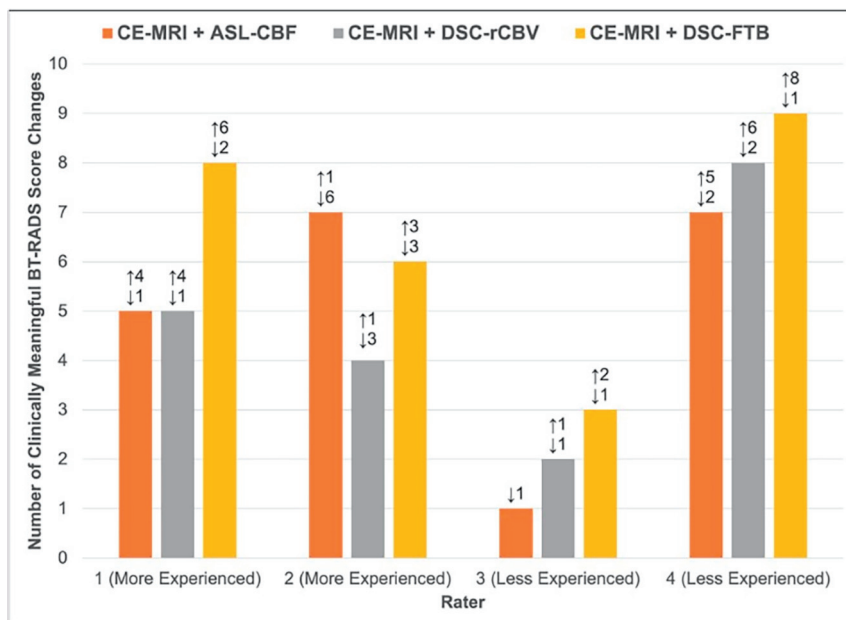


**FIG 3.** Clinically meaningful changes in BT-RADS scores following the inclusion of perfusion metrics compared with conventional CE-MR imaging alone. Clinically meaningful upgrades or downgrades were defined as score changes from  $\leq 3a \leftrightarrow 3b$  or  $3b \leftrightarrow 3c/4$  and from  $3c/4 \leftrightarrow \leq 3b$  or  $3b \leftrightarrow \leq 3a$ , respectively. The numbers and arrows above the bar graph indicate the number of score upgrades (upward facing arrow) or downgrades (downward facing arrow). The greatest number of score changes was observed with the addition of DSC-FTB.

### Confidence in MR Imaging Interpretations

Confidence scores for all raters, regardless of experience, were higher with the addition of perfusion metrics and were highest with FTB. Figure 4 shows the frequency and mean of scores. For raters 1, 2, and 3, there were no significant differences in confidence scores among CE-MR imaging, CE-MR imaging+ASL-CBF, CE-MR imaging+DSC-rCBV, and CE-MR imaging+DSC-FTB ( $P = .195, .052$ , and  $.540$ , respectively). For rater 4, a significant difference in confidence scores was detected among the metrics assessed ( $P = .001$ ). Pair-wise comparisons revealed significant differences between CE-MR imaging and CE-MR imaging+DSC-rCBV and between CE-MR imaging and CE-MR imaging+DSC-FTB (adjusted  $P = .005$ , and  $< .001$ , respectively). No other differences were significant.

### DISCUSSION

Our study demonstrates that the addition of perfusion metrics to conventional CE-MR imaging resulted in higher agreement and confidence in neuroradiologists' clinical interpretation of post-treatment MR imaging of HGGs. Among the perfusion metrics evaluated in this study—ASL-CBF, DSC-rCBV, and DSC-FTB—the highest agreement and confidence were seen with DSC-FTB, a relatively newer described metric in brain tumor imaging. Moreover, our study found that the addition of perfusion metrics to CE-MR imaging yielded clinically meaningful changes in MR imaging interpretation that could affect management in up to 20% of patients compared with the use of CE-MR imaging alone.

Adding perfusion metrics to conventional CE-MR imaging resulted in higher IRA in BT-RADS scores compared with CE-

MR imaging alone in this study. Prior studies have similarly shown that adding perfusion metrics to CE-MR imaging can increase the IRA. Maiter et al<sup>18</sup> showed fair agreement among raters ( $\kappa = 0.58$ ) when rCBV maps were qualitatively assessed with conventional MR imaging in posttreatment gliomas. Kerkhof et al<sup>19</sup> found good interobserver agreement ( $\kappa = 0.63$ ) on the visual assessment of rCBV maps in GBM as being high or low, though agreement on the overall tumor status was lower ( $\kappa = 0.48$ ). While the IRA improved with the addition of all 3 perfusion metrics, the highest agreement was seen with DSC-FTB, which was not evaluated in previous studies. Even agreement between a multidisciplinary consensus group and raters, despite years of experience, was consistently the highest with DSC-FTB, indicating that this metric may improve the clarity of interpretation. In DSC-FTB, the contrast-enhancing volume is classified into areas of the likelihood of tumor burden based on

predefined rCBV thresholds, which are used to color-code the images for ease of interpretation. This step removes some of the subjectivity inherent in qualitative image interpretation and accounts for the greater agreement seen with DSC-FTB compared with ASL-CBF and DSC-rCBV, particularly in lesions that have an admixture of tumor and treatment effect.

Furthermore, our results show that clinically meaningful changes in interpretation following the use of any perfusion metric, which, in practice, may result in a change in therapeutic management, occurred in up to 20% of patients compared with the use of CE-MR imaging alone. These results are similar to those in previous studies showing the potential of perfusion MR imaging to influence patient management. Geer et al<sup>10</sup> evaluated the impact of DSC and ASL on clinical management in patients with gliomas and found that the addition of perfusion imaging was associated with a change in management plan in up to 8.5% of patients. Maiter et al<sup>18</sup> showed that rCBV<sub>mean</sub> ratios in GBM changed the interpretation in 6.3% of reports among readers. Yang et al<sup>20</sup> demonstrated that the addition of DSC PWI-derived rCBV<sub>max</sub> (and DWI) improved the diagnostic performance for distinguishing recurrent GBM from nonrecurrence in BT-RADS category 3 lesions. Iv et al<sup>9</sup> showed that FTB can help distinguish recurrent GBM from treatment effects and guide clinical decision-making in posttreatment GBMs. In our study, while no significance was found among the various perfusion metrics with respect to the number of clinically meaningful score changes, the greatest number of changes was seen with DSC-FTB in 3 of the 4 raters. The absence of statistical significance may, in part, be related to our small sample size, but these findings have important implications when taken on an individual patient level.



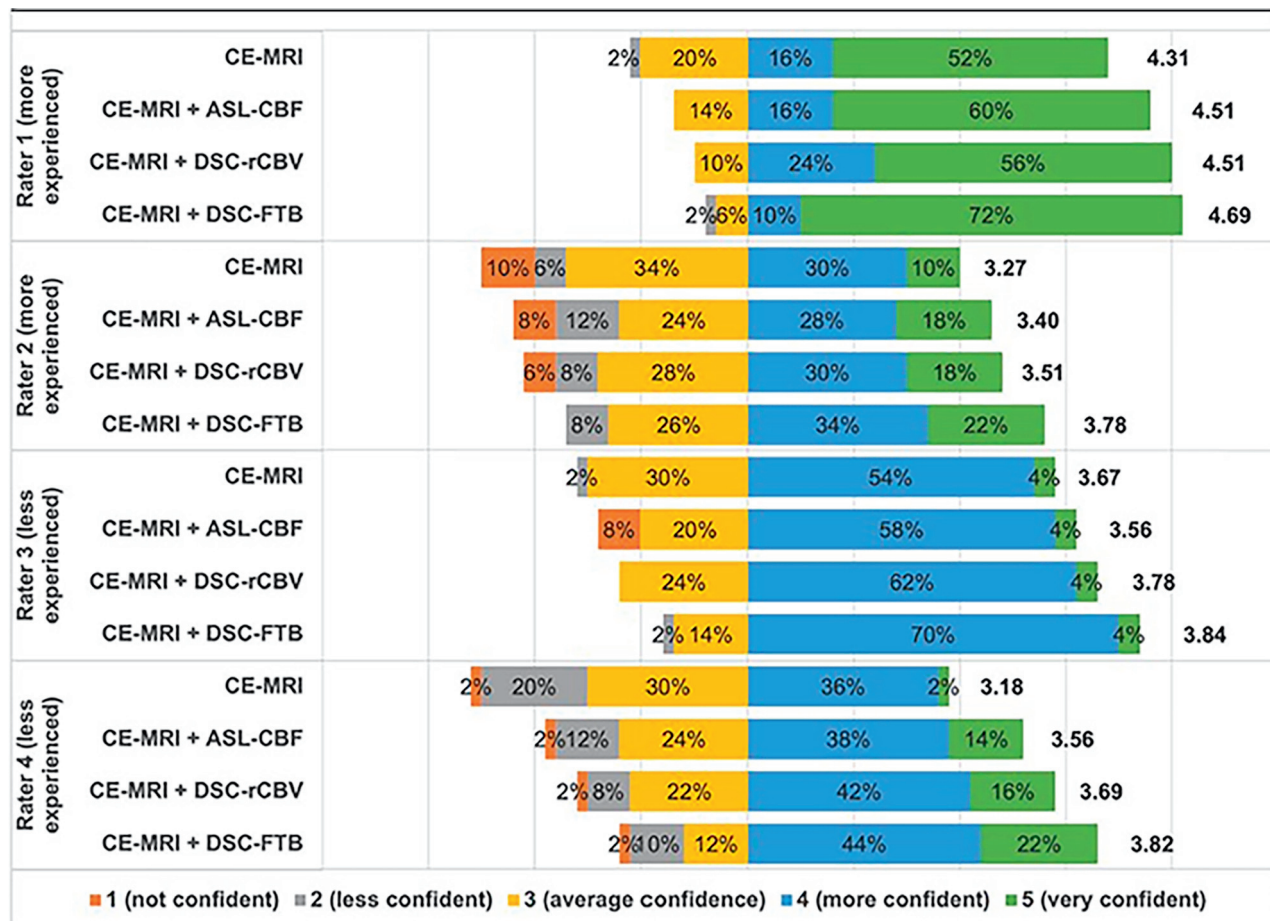


**FIG 4.** Rater confidence in MR imaging interpretation. Raters graded their confidence in interpretation and assignment of BT-RADS scores for conventional CE-MR imaging, CE-MR imaging + ASL-CBF, CE-MR imaging + DSC-rCBV, and CE-MR imaging + DSC-FTB using a 5-point Likert scale. The number to the right of each color bar represents the mean score. In general, confidence was higher with the addition of any perfusion metric but was highest with DSC-FTB in all raters.

Finally, we found that perfusion MR imaging resulted in higher confidence in interpretation, which has also been demonstrated in other studies. Maiter et al<sup>18</sup> showed an 11.5% increased confidence in the overall opinion of GBM status (progression, pseudoprogression, mixed, or indeterminate) with rCBV<sub>mean</sub> ratios. Geer et al<sup>10</sup> showed that the addition of DSC or ASL to CE-MR imaging increased treatment confidence in the management plan in 57.6% of patient episodes. In this study, the addition of DSC-rCBV and DSC-FTB to CE-MR imaging increased the confidence in interpretation for one of the less experienced raters. Despite no significance found in confidence scores among CE-MR imaging, CE-MR imaging+ASL-CBF, CE-MR imaging+DSC-rCBV, and CE-MR imaging+DSC-FTB for the other 3 raters, scores were generally higher with the addition of perfusion metrics across all raters and were highest with DSC-FTB despite varying experience years.

Although several studies have shown the value of perfusion imaging in the identification of tumor progression and treatment effect, perfusion imaging is still not widely adopted for this patient population at many centers. This study shows the value of adding any perfusion metric, whether derived from ASL or DSC, to conventional CE-MR imaging for routine posttreatment HGG surveillance imaging, not only when there is a concern for tumor

progression or pseudoprogression, and supports its inclusion in a standard glioma MR imaging protocol. Whereas prior studies have primarily looked at ASL-CBF and DSC-rCBV, this study also evaluated the recently described DSC-FTB metric, which incorporates quantitative rCBV thresholds, and shows that it provides better interrater agreement and higher confidence scores in routine interpretation, in large part because FTB maps are typically easier to interpret. Thus, our study demonstrates the clinical translation and integration of quantitative perfusion markers in neuro-oncology imaging and their value in day-to-day clinical practice.

Some important limitations in this study must be considered. One limitation is the lack of histopathologic confirmation to establish a “ground truth” for most cases. In the clinical setting, however, histopathology is not available at each imaging timepoint and, most important, it is not always required for treatment decisions to be made. We, instead, used an experienced consensus group as our reference standard, as used in similar clinical imaging studies<sup>18</sup> and in real-time practice. Another limitation of this study is the small sample size. While DSC-FTB resulted in a greater number of clinically meaningful changes in BT-RADS scores than ASL-CBF and DSC-rCBV, a larger study must be undertaken to determine whether this change holds true. While most patients undergoing surveillance MR imaging for posttreatment HGG can



receive gadolinium-based contrast, some cannot. A future study can evaluate how the addition of ASL-CBF to noncontrast MR imaging influences the interpretation of posttreatment HGG in patients who cannot receive contrast. Finally, given the retrospective nature of the study, there was some variation in MR imaging techniques within the same patient and between patients. However, this reflects real-life clinical practice in which ensuring homogeneity in image acquisition across patients and timepoints is challenging, if not impossible.

## CONCLUSIONS

Adding ASL-CBF, DSC-rCBV, and DSC-FTB to conventional CE-MR imaging improves the IRA in neuroradiologists' clinical interpretations of posttreatment MR imaging of HGGs. Of the perfusion metrics evaluated, DSC-FTB resulted in the highest agreement in BT-RADS scores among all raters and between an experienced multidisciplinary consensus group and individual raters regardless of practice experience years. The addition of perfusion metrics also resulted in higher confidence in interpretation, with the highest scores seen with DSC-FTB, and yielded potential clinically meaningful changes in MR imaging interpretation in up to 20% of patients. Our results highlight the value of adding perfusion imaging to a standard glioma MR imaging protocol for routine interpretation of posttreatment HGGs. Of the perfusion metrics analyzed, DSC-FTB may provide the most benefit regarding multireader agreement and confidence in interpretation, which may be helpful in those with less experience in neuro-oncology imaging.

**Disclosure forms** provided by the authors are available with the full text and PDF of this article at [www.ajnr.org](http://www.ajnr.org).

## REFERENCES

- Wen PY, Macdonald DR, Reardon DA, et al. **Updated response assessment criteria for high-grade gliomas: Response Assessment in Neuro-Oncology Working Group.** *J Clin Oncol* 2010;28:1963–72 [CrossRef Medline](#)
- Weinberg BD, Gore A, Shu HG, et al. **Management-based structured reporting of posttreatment glioma response with the Brain Tumor Reporting and Data System.** *J Am Coll Radiology* 2018;15:767–71 [CrossRef Medline](#)
- Barajas RF Jr, Chang JS, Segal MR, et al. **Differentiation of recurrent glioblastoma multiforme from radiation necrosis after external beam radiation therapy with dynamic susceptibility-weighted contrast-enhanced perfusion MR imaging.** *Radiology* 2009;253:486–96 [CrossRef Medline](#)
- Hu LS, Baxter LC, Smith KA, et al. **Relative cerebral blood volume values to differentiate high-grade glioma recurrence from post-treatment radiation effect: direct correlation between image-guided tissue histopathology and localized dynamic susceptibility-weighted contrast-enhanced perfusion MR imaging measurements.** *AJNR Am J Neuroradiol* 2009;30:552–58 [CrossRef Medline](#)
- Prager AJ, Martinez N, Beal K, et al. **Diffusion and perfusion MRI to differentiate treatment-related changes including pseudoprogression from recurrent tumors in high-grade gliomas with histopathologic evidence.** *AJNR Am J Neuroradiol* 2015;36:877–85 [CrossRef Medline](#)
- Ozsunar Y, Mullins ME, Kwong K, et al. **Glioma recurrence versus radiation necrosis? A pilot comparison of arterial spin-labeled, dynamic susceptibility contrast enhanced MRI, and FDG-PET imaging.** *Acad Radiol* 2010;17:282–90 [CrossRef Medline](#)
- Liu Y, Chen G, Tang H, et al. **Systematic review and meta-analysis of arterial spin-labeling imaging to distinguish between glioma recurrence and post-treatment radiation effect.** *Ann Palliat Med* 2021;10:12488–97 [CrossRef Medline](#)
- Nguyen TB, Zakhari N, Velasco Sandoval S, et al. **Diagnostic accuracy of arterial spin-labeling, dynamic contrast-enhanced, and DSC perfusion imaging in the diagnosis of recurrent high-grade gliomas: a prospective study.** *AJNR Am J Neuroradiol* 2023;44:134–42 [CrossRef Medline](#)
- Iv M, Liu X, Lavezo J, et al. **Perfusion MRI-based fractional tumor burden differentiates between tumor and treatment effect in recurrent glioblastomas and informs clinical decision-making.** *AJNR Am J Neuroradiol* 2019;40:1649–57 [CrossRef Medline](#)
- Geer CP, Simonds J, Anvery A, et al. **Does MR perfusion imaging impact management decisions for patients with brain tumors? A prospective study.** *AJNR Am J Neuroradiol* 2012;33:556–62 [CrossRef Medline](#)
- Hu LS, Baxter LC, Pinnaduwa DS, et al. **Optimized preload leakage-correction methods to improve the diagnostic accuracy of dynamic susceptibility-weighted contrast-enhanced perfusion MR imaging in posttreatment gliomas.** *AJNR Am J Neuroradiol* 2010;31:40–48 [CrossRef Medline](#)
- Schminda KM, Prah MA, Rand SD, et al. **Multisite concordance of DSC-MRI analysis for brain tumors: results of a National Cancer Institute Quantitative Imaging Network collaborative project.** *AJNR Am J Neuroradiol* 2018;39:1008–16 [CrossRef Medline](#)
- Schminda KM, Prah MA, Hu LS, et al. **Moving toward a consensus DSC-MRI protocol: validation of a low-flip angle single-dose option as a reference standard for brain tumors.** *AJNR Am J Neuroradiol* 2019;40:626–33 [CrossRef Medline](#)
- Prah MA, Al-Gizawi MM, Mueller WM, et al. **Spatial discrimination of glioblastoma and treatment effect with histologically-validated perfusion and diffusion magnetic resonance imaging metrics.** *J Neurooncol* 2018;136:13–21 [CrossRef Medline](#)
- Hu LS, Kelm Z, Korfiatis P, et al. **Impact of software modeling on the accuracy of perfusion MRI in glioma.** *AJNR Am J Neuroradiol* 2015;36:2242–49 [CrossRef Medline](#)
- Hu LS, Eschbacher JM, Heiserman JE, et al. **Reevaluating the imaging definition of tumor progression: perfusion MRI quantifies recurrent glioblastoma tumor fraction, pseudoprogression, and radiation necrosis to predict survival.** *Neuro Oncol* 2012;14:919–30 [CrossRef Medline](#)
- Connelly JM, Prah MA, Santos-Pinheiro F, et al. **Magnetic resonance imaging mapping of brain tumor burden: clinical implications for neurosurgical management: case report.** *Neurosurg Open* 2021;2:okab029 [CrossRef Medline](#)
- Maiter A, Butteriss D, English P, et al. **Assessing the diagnostic accuracy and interobserver agreement of MRI perfusion in differentiating disease progression and pseudoprogression following treatment for glioblastoma in a tertiary UK centre.** *Clin Radiol* 2022;77:e568–75 [CrossRef Medline](#)
- Kerkhof M, Hagenbeek RE, van der Kallen BF, et al. **Interobserver variability in the radiological assessment of magnetic resonance imaging (MRI) including perfusion MRI in glioblastoma multiforme.** *Eur J Neurol* 2016;23:1528–33 [CrossRef Medline](#)
- Yang Y, Yang Y, Wu X, et al. **Adding DSC PWI and DWI to BT-RADS can help identify postoperative recurrence in patients with high-grade gliomas.** *J Neurooncol* 2020;146:363–71 [CrossRef Medline](#)